Acta Geodyn. Geomater., Vol. 4, No. 1 (145), 67-75, 2007

MONITORING ACTIVE STRUCTURES IN EASTERN CORINTH GULF (GREECE): THE KAPARELLI FAULT

Athanassios GANAS [1)]*, Jaroslaw BOSY [2)], Lubomir PETRO [3)], George DRAKATOS [1),] Bernard KONTNY [2)], Marian STERCZ [3)], Nikolaos S. MELIS [1)], Stefan CACON [2)] and Anastasia KIRATZI [4)]

[1)] *National Observatory of Athens, Geodynamic Institute, Lofos Nymfon, Athens 118 10, Greece*
[2] *Institute of Geodesy and Geoinformatics, Wroclaw University of Environmental and Life Sciences, Grunwaldzka 53, 50-357 Wroclaw, Poland*
[3)] *Geological Survey of Slovak Republic, Jesenskeho 8, SK-040 01 Kosice, Slovak Republic*
[4)] *Department of Geophysics, Aristotle University of Thessaloniki, 54124 Thessaloniki, Greece*
**Corresponding author's e-mail*: aganas@gein.noa.gr

(*Received* January 2007, *accepted* March 2007)

ABSTRACT
A collaborative group between Greek, Polish, and Slovak colleagues installed a dense network of non-permanent GPS stations and extensometers to monitor active faults in the eastern part of the Gulf of Corinth, central Greece. The network includes eleven GPS stations across the Kaparelli fault and the Asopos rift valley to the east and two TM-71 extensometers that were installed on the Kaparelli fault plane. So far the GPS network has been measured in three campaigns within the last three years with very good accuracies (1-4 mm in the horizontal plane). Although it is early to draw conclusions on the velocity field and on strain patterns it can be noted that, the data from the extensometers demonstrate both fault-normal opening and shear motion. Given that the total offset on the Kaparelli fault is small, and the geological data suggesting a segmented character of this fault, we expect in the near future to differentiate fault slip and strain accumulation among segments.

KEYWORDS: active faults, GPS, TM-71, Kaparelli, Corinth Gulf, earthquakes, strain

1. INTRODUCTION

The Gulf of Corinth in central Greece is one of the most tectonically active and rapidly extending regions in the world. Surface topography and geomorphology are clearly associated with seismic activity along large normal faults (Armijo et al., 1996). Extension is mainly directed N-S (Clarke et al. 1998). The southern side of the Gulf of Corinth is bound by a series of major north-dipping normal faults, forming a complex asymmetric half graben (Jackson et al., 1982). There are E-W striking normal faults with antithetic dip, i.e. to the south; however, they are visible at the northern edge of the Gulf.

In February – March 1981 a sequence of three earthquakes with magnitudes greater than 6.3 struck the eastern Gulf of Corinth (Hubert et al., 1996). North-dipping surface breaks were noted the morning after the first two events on the southern side of the Gulf (Perachora Peninsula) and south-dipping ruptures appeared on the northern side of the Gulf (Kaparelli region) as a result of the third event (Figure 1; data from Jackson et al., 1982). In both areas seismic motion occurred along basin-bounding faults bringing in contact Mesozoic limestone and alluvial deposits as well as colluvium.

Focal mechanisms of small and shallow earthquakes (data from Ambraseys and Jackson, 1990) also show normal faulting with the active fault plane dipping at about 45° for faults at the eastern end of the Gulf of Corinth including Kaparelli. Recently, three trenches have been excavated across the Kaparelli Fault (Pavlides et al., 2003; Kokkalas et al., in press). Their stratigraphic record shows at least three events during the Holocene period, with the 1981 event included. The estimated mean slip rate is 0.28 mm/yr. Colluvial tectonostratigraphy and analysis of displacements on key horizons suggests surface rupturing events in the order of 0.7-1 m.

The Kaparelli Fault consists of three segments, two of which were ruptured in 1981 (Jackson et al., 1982). The two-ruptured segments form left-stepping en echelon geometry, while the third north-western segment of the fault did not rupture (Figure 2). The fault segments are clearly expressed at the surface by nearly continuous scarps. The footwall elevation is 600 m and lithology is composed of hard, Mesozoic limestone. The hanging wall block forms a small basin and contains approximately 200 m of fluvial-terrestrial deposits of Pleistocene age as well as Holocene alluvium.

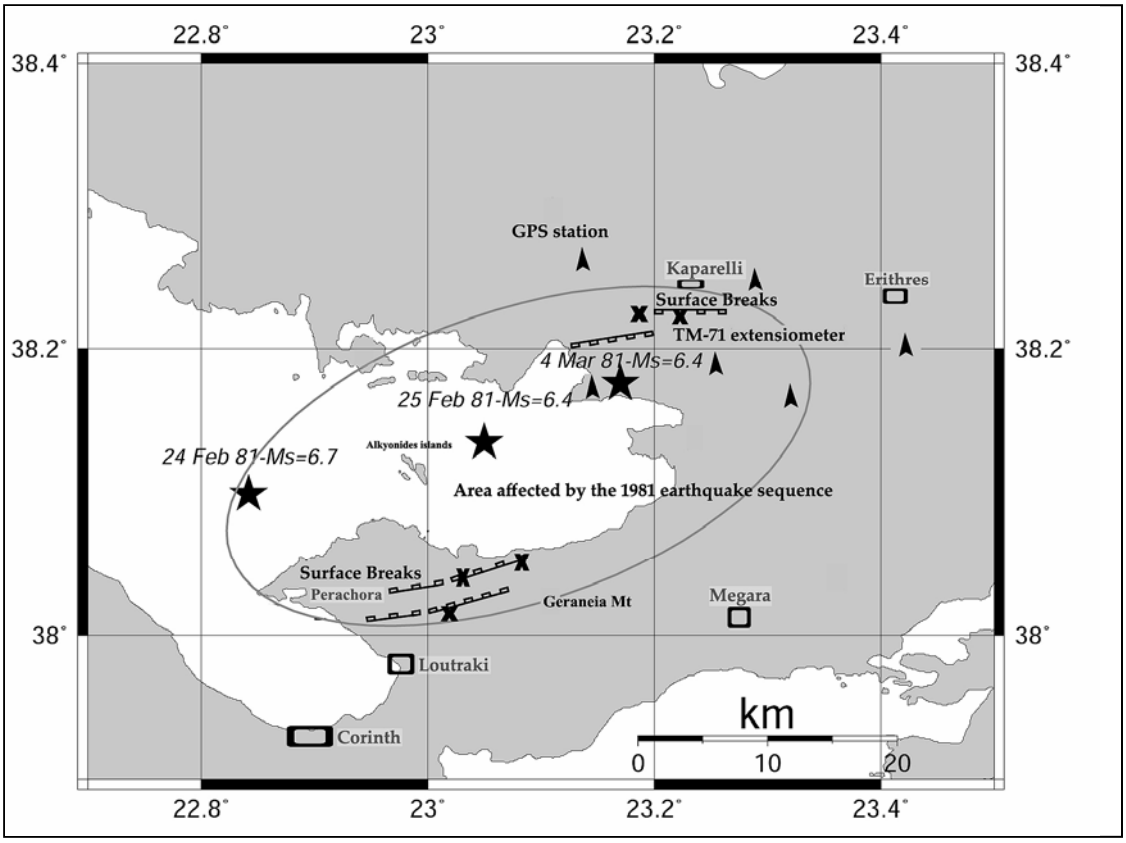

Fig. 1 Map of the study area showing epicentres of the 1981 earthquake sequence (stars). X signs point to TM-71 instrument locations and black arrows indicate locations of non-permanent GPS stations established during 2003. Lines with barbs indicate normal faults that ruptured during the 1981 earthquake sequence.

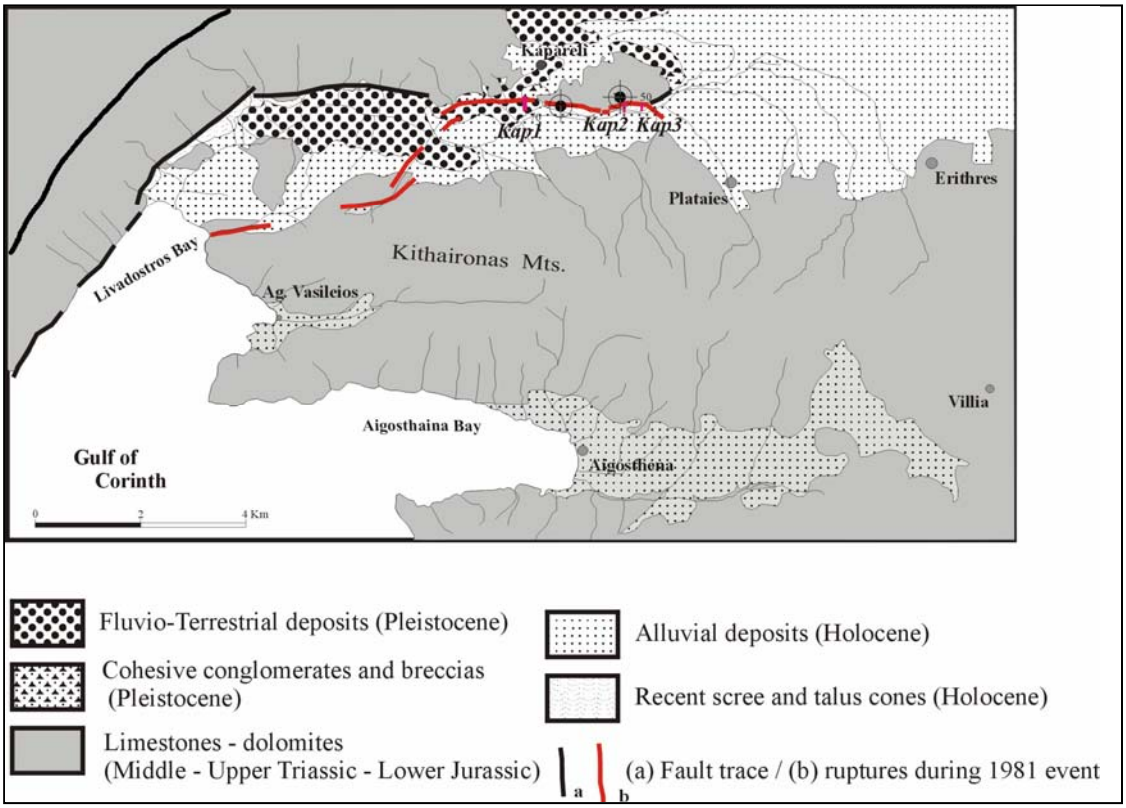

Fig. 2 Geological map of the Kaparelli area in central Greece. The 1981 ruptures are shown in light grey. Trench positions are denoted by *Kap1*, *Kap2* and *Kap3*. Circle symbols point to TM-71 installations. Map after Pavlides et al., 2003.

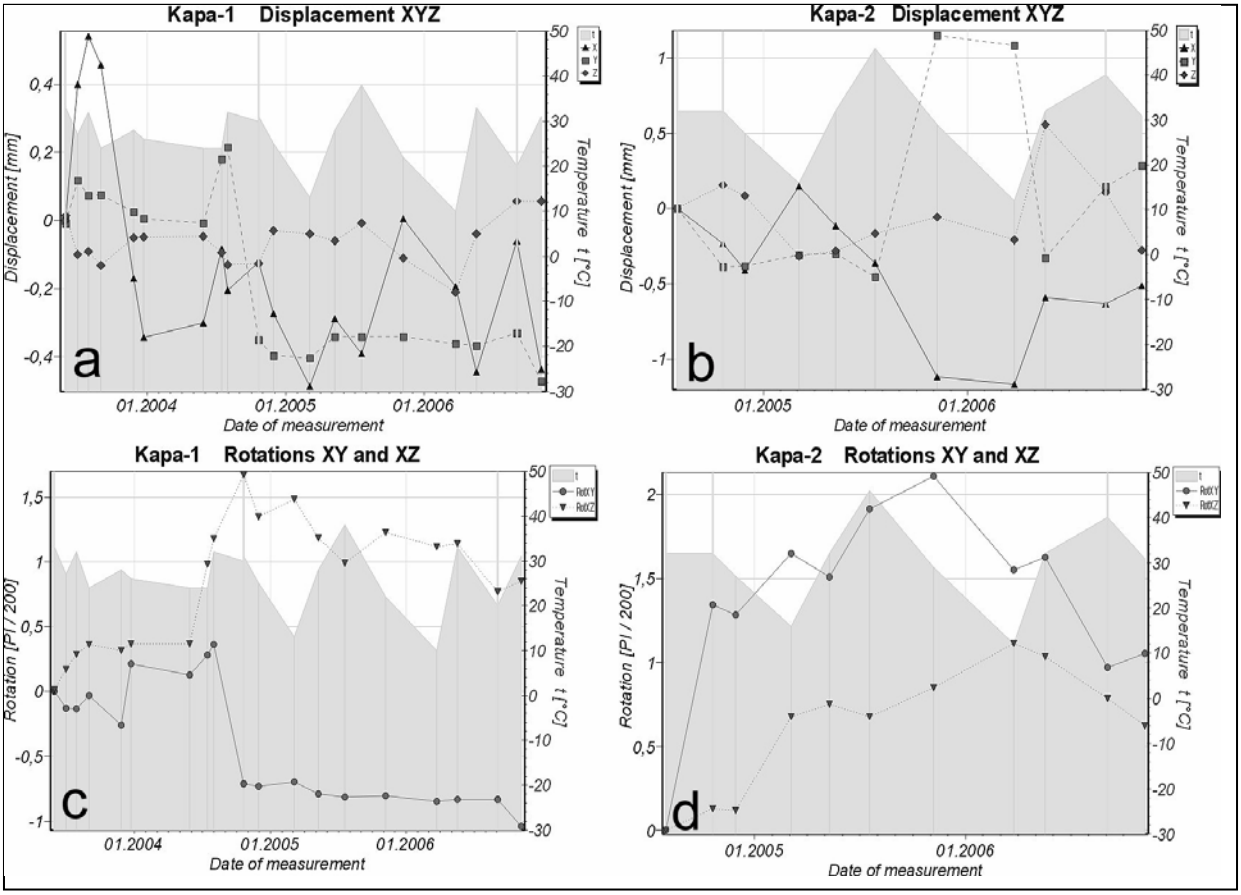

Fig. 3 (a) Displacement – Time diagram for site Kapa1. +x indicates contraction of distance between walls. +y means displacement of the hanging wall to the East; +z means subsidence of the hanging wall (uplifting the foot wall).
(b) Diagram for site Kapa2. Bottom graphs
(c) & (d) show rotation of XY (horizontal) and XZ (vertical) planes of the instrument, respectively. Units are in grades (1 circle = 400 grades). We observe that point Kapa1 shows XY rotations of approx -0.8 grades and similarly XZ rotations around +1.2 grades in the second half of 2004 which is in agreement with fault kinematics (dextral shear motion)

2. MONITORING THE ACTIVITY OF THE KAPARELLI FAULT

In order to measure the kinematics of deformation in 3-D the Greek group together with the Polish and Slovak groups, have established a dense GPS network and two (2) extensometers. The details of installation of instruments and project rationale are given in Drakatos et al. (2005) and Cacon et al. (2005). In summary, the Slovakian and Greek groups have begun monitoring the Kaparelli fault area since May 2003. On May 26, 2003 they installed an extensometer of TM-71 type (Košťák and Cruden, 1990). A second instrument was installed on July 15, 2004. In addition, a dense GPS network has been installed within a collaboration of Greek and Polish groups, comprising six (6) stations. The network was deployed on November, 11-12 2003 and its first measurement took place in May 2004. The network was expanded on March 31, 2005. Five (5) new stations were installed inside the Asopos rift valley (see Figure 4 below). Both sub-networks were measured during May 2005 and May 2006.

3. MONITORING FAULT MOTION USING TM-71 INSTRUMENTS

The 2003 installation of observation point Kapa1 was done at the trench Kap2 that was excavated across the fault (Figure 2; Pavlides et al., 2003). The TM-71 is fixed to the fault (north side) and to a construction built on the hanging wall (south side) by steel bars. The 2004 installation of Kapa2 was done against a free surface of the fault plane, about 2 km to the west of locality Kap2. The position of the X, Y, and Z axes of the instrument corresponds respectively to: (X) the direction perpendicular to the fault or fault-normal motion, (Y) direction parallel to fault strike or the strike slip motion along the fault surface and (Z) vertical direction or the dip slip component of motion.

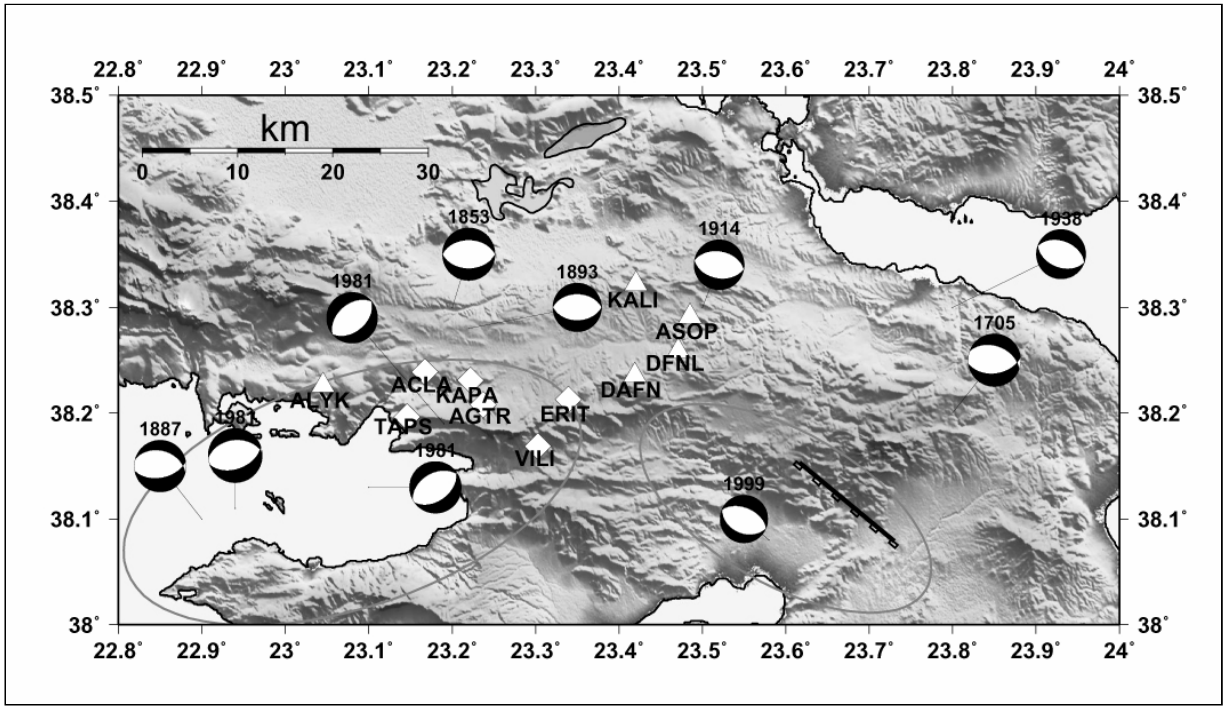

Fig. 4 Shaded relief map of the study area showing the locations of the GPS stations. White Diamonds show the 2003 points and triangles the 2005 points, respectively. Beachballs represent fault plane solutions of strong, shallow earthquakes. Ellipses mark the rupture zones of the 1981 and 1999 earthquakes, respectively.

The instrument readings are recorded on a nearly monthly basis by NOA. Our observations for the site Kapa1 span a period of 3 years so it is possible to make a preliminary interpretation (Figure 3). From November 2003 the course in Kapa1 X-axis shows variations ±0.25 mm which can be attributed to seasonal temperature variations upon rock and is normal with this type of measurement (Drakatos et al., 2005). An extreme was observed between May and August 2003, (+0.5 mm) followed by a back-movement of -0.85 mm. This occurred in the initial period of measurement when a concrete block settlement after its creation inside the trench may be present. Since 2004 we observe continuous opening that is in agreement with fault kinematics. Displacement along Z-axis is relatively stable. Along the axis Y (horizontal; along the fault strike) observed motion is dextral oblique slip of -0.6 mm between June and November 2004 followed by relative stability. It is interesting to see that a similar pattern was observed in the rotation plots (Figure 3c) for the planes XY (the horizontal plane) and XZ (the vertical plane). Records show change at the same time in the second half of 2004, after which stability re-established. This dextral shear motion is consistent with the slip vector model of Roberts and Ganas (2000) that predict oblique slip vectors at normal fault tips. At Kapa2 the observation period is only two years (X-axis; Figure 3b) and the record needs more time to be interpreted.

4. MONITORING REGIONAL DEFORMATION USING GPS INSTRUMENTS

The motion of crustal blocks in central Greece can be described in a first approximation by a combination of translation and rotation (Goldsworthy et al., 2002). By combining the displacement vectors obtained at points of successive GPS campaigns during 2004-2006 and later, we will compute the velocity field over a distance of 30 km (E-W). The network was measured for the first time in May 2004 using the ASTHECH receivers of the Polish group. In particular stations ERIT, KAPA and TAPS (Figure 4) were observed using ASHTECH Zxtreme instruments and ASH701975.01A antennas while the remaining stations were observed using Z-XII instruments and ASH700718B antennas. Station AGTR (Figure 4) was used as the base station. The initial network was expanded during 2005 with the installation of five (5) more stations. All NOA stations were measured using Leica 1200 receivers.

The GPS observations from 2005 and 2006 campaigns were processed in ITRF2000 (Altamini et al., 2002) frame (each daily session separately) using as fiducial points the IGS Italian Permanent Station Matera (MATE) and Greek stations: IGD1 in 2005 and NOA1 in 2006. The Bernese GPS Software v. 4.2 (Hugentobler et al., 2001) was used and special data processing strategy was developed for the local precise network with the following issues and

Table 1 Parameters of the KAPNET GPS antennas during the 2005 (DOY 130, 131) and 2006 (DOY 122, 123) observation campaigns. Height is in metres.

2005							
130				131			
POINT	**ANT. TYPE**	**h-OBS**	**h-RED**	**POINT**	**ANT. TYPE**	**h-OBS**	**h-RED**
ACLA	ASH700718B	0.8290	0.7654	ACLA	ASH700718B	0.8300	0.7664
AGTR	ASH700936D_M	0.7640	0.7262	AGTR	ASH700936D_M	0.7640	0.7262
ERIT	ASH701975.01Agp	0.7810	0.7380	ERIT	ASH701975.01Agp	0.7830	0.7400
KAPA	ASH701975.01Agp	0.8080	0.7650	KAPA	ASH701975.01Agp	0.8070	0.7640
TAPS	ASH701975.01Agp	0.8140	0.7710	TAPS	ASH701975.01Agp	0.8140	0.7710
VILI	ASH700718B	0.8150	0.7514	VILI	ASH700718B	0.8150	0.7514
ALYK	LEIAT502	0.7230	0.6672	ALYK	LEIAT502	0.7230	0.6672
ASOP	LEIAX1202	0.7500	0.6880	ASOP	LEIAX1202	0.7500	0.6880
DAFN	LEIAX1202	0.7210	0.6590	DAFN	LEIAX1202	0.7210	0.6590
DFNL	LEIAX1202	0.7390	0.6770	DFNL	LEIAX1202	0.7390	0.6770
KALI	LEIAX1202	0.7230	0.6610	KALI	LEIAX1202	0.7230	0.6610
2006							
122				123			
POINT	**ANT. TYPE**	**h-OBS**	**h-RED**	**POINT**	**ANT. TYPE**	**h-OBS**	**h-RED**
ACLA	ASH700718B	0.8350	0.7714	ACLA	ASH700718B	0.8350	0.7714
AGTR	ASH700936D_M	0.7640	0.7292	AGTR	ASH700936D_M	0.7640	0.7292
ERIT	ASH701975.01Agp	0.7810	0.7380	ERIT	ASH701975.01Agp	0.7810	0.7380
KAPA	ASH701975.01Agp	0.8070	0.7640	KAPA	ASH701975.01Agp	0.8070	0.7640
TAPS	ASH701975.01Agp	0.8120	0.7690	TAPS	ASH701975.01Agp	0.8120	0.7690
VILI	ASH700718B	0.8200	0.7564	VILI	ASH700718B	0.8210	0.7574
ALYK	LEIAT502	0.6910	0.6910	ALYK	LEIAT502	0.6910	0.6910
ASOP	LEIAX1202	0.6910	0.6910	ASOP	LEIAX1202	0.6910	0.6910
DAFN	LEIAX1202	0.6910	0.6910	DAFN	LEIAX1202	0.6910	0.6910
DFNL	LEIAX1202	0.6910	0.6910	DFNL	LEIAX1202	0.6910	0.6910
KALI	LEIAT502	0.6910	0.6910	KALI	LEIAT502	0.6910	0.6910

assumptions (Bosy and Kontny, 1998; Bosy et al., 2003):

- Global ionosphere model CODE for a phase ambiguity resolution,
- Antenna phase centres calibrated according to the NGS,
- Troposphere model – the Niell mapping function without a priori model; residual atmosphere zenith delays were estimated for one-hour intervals,
- Precise ephemeris computed by the Centre of Orbit Determination in Europe (CODE) to determine satellite positional data.

All KAPNET positions were resolved with Root-Mean-Square residuals less than 5 mm (horizontal plane; Figure 5). The antenna parameters of the 2005 campaign are given in Table 1. Table 2 presents the ITRF 2000 coordinates of all stations. Figure 5 shows the RMS (Root Mean Square) residuals of the station solutions.

Our first results include coordinates and RMS errors of KAPARELLI local network points for two years 2005 and 2006. They were generated by connecting the daily solutions using the ADDNEQ program (Brockmann, 1996; Hugentobler et al., 2001). Computed ITRF2000 geodetic coordinates (φ, λ h) referring to their respective epochs as well as their RMS errors are provided in Table 2. The accuracy of determined coordinates (φ, λ and h) representing un-weighted RMS values of coordinate residuals taken from each year (comparison of station coordinates from each session with respect to the combined solution in mm) is shown in Figure 5. The un-weighted RMS values computed from repeated observations give more realistic accuracy of stations coordinates. The organisation and data processing of repeated satellite GPS standards provide conditions for detecting horizontal movements of the stations at the <5 mm level.

5. DISCUSSION - CONCLUSIONS

a) Dextral shear motion at Kapa1 was indicated. This is found in agreement with non-uniform strain patterns along active normal faults (Roberts and Ganas, 2000). Besides, till now, the TM71

Table 2 The ITRF 2000 coordinates of the KAPNET stations

Point	φ			λ			h	RMS φ	RMS λ	RMS h
	[o ' "]			[o ' "]			[m]	[mm]	[mm]	[mm]
ITRF2000 EPOCH: 2005-05-10 23:59:45										
ACLA	38	14	20.457830	23	10	1.655841	473.2161	0.5	0.7	3.7
AGTR	38	12	29.119021	23	14	13.982700	578.4204	0.5	0.7	3.7
ALYK	38	13	34.536100	23	2	42.984761	474.9853	0.7	0.7	4.9
ASOP	38	17	28.851765	23	29	6.323049	321.9817	0.5	0.7	3.7
DAFN	38	14	8.585989	23	25	7.455789	533.3963	0.5	0.7	3.7
DFNL	38	15	31.194095	23	28	16.535688	357.5885	0.5	0.7	3.7
ERIT	38	12	47.859336	23	20	21.377514	474.0419	0.5	0.7	3.9
KALI	38	19	18.825944	23	25	14.223037	395.7988	0.5	0.7	3.9
KAPA	38	13	52.699457	23	13	18.760112	340.7526	0.5	0.7	3.7
TAPS	38	11	47.745238	23	8	45.103563	481.9591	0.5	0.7	3.9
VILI	38	10	7.788711	23	18	11.234132	694.3970	0.5	0.7	3.7
ITRF2000 EPOCH: 2006-05-02 23:59:45										
ACLA	38	14	20.457462	23	10	1.656128	473.2449	0.5	0.5	3.1
AGTR	38	12	29.118592	23	14	13.982988	578.4606	0.3	0.3	2.0
ALYK	38	13	34.535574	23	2	42.985050	475.0196	0.4	0.5	3.0
ASOP	38	17	28.851322	23	29	6.323437	322.0029	0.3	0.4	2.3
DAFN	38	14	8.585571	23	25	7.456152	533.3879	0.4	0.5	2.7
DFNL	38	15	31.193592	23	28	16.535760	357.6028	0.3	0.4	2.1
ERIT	38	12	47.858913	23	20	21.377813	474.0702	0.3	0.4	2.1
KALI	38	19	18.825917	23	25	14.223237	395.8117	0.3	0.4	2.7
KAPA	38	13	52.699048	23	13	18.760358	340.7809	0.4	0.4	2.4
TAPS	38	11	47.744646	23	8	45.103803	481.9939	0.3	0.4	2.1
VILI	38	10	7.788286	23	18	11.234429	694.4191	0.3	0.3	2.0

instruments along the Kaparelli Fault show seasonal effects (Figure 3) compatible with seasonal temperature variation.

b) Three (3) similar instruments have been installed in the Perachora peninsula by Maniatis et al. (2003; Figure 1). Given that Holocene fault slip rates at these localities differ by a factor of five (5) or even more it is important to compare 3-D strain measurements in order to estimate inter-seismic strain accumulation along the two fault zones. Another issue concerns the identification of instrument-induced errors on our measurements and their estimation. The advantage that TM-71 has no electronics parts is counterbalanced by the infinitesimal deformations caused by climatic fluctuations (precipitation, temperature). For example a seasonal effect along the X-axis is visible in the 16-year data series from the Simitli graben in SW Bulgaria (Dobrev and Košťák, 2000).

c) The data processing of repeated satellite GPS standards provide conditions for detecting horizontal movements at our stations at 2-4 mm level. Taking into account the fault movement rate of about 0.5 mm/y, indicated by TM-71 (Figure 3), significant displacement across Kaparelli can be detected by GPS after 4-5 years of observations.

d) The large E-W faults of the Gulf of Corinth slip fast (1-2 mm/yr) and terminate towards the south of the Kaparelli Fault, while the large normal faults of the Parnitha region to the east slip at about five (5) to ten (10) times less (0.2-0.4 mm/yr; Ganas et al., 2004). It is interesting to map this transition in fault slip rates by using the GPS measurements of KAPNET. Our first results (Figure 5) point to an excellent quality of GPS data that will provide stable solutions. A second point concerns the total offset on the Kaparelli fault that is small (< 200 m), while the geological data suggest that it is segmented. So our GPS measurements will differentiate fault slip and strain accumulation among the segments. These observations will also shed light into fault growth processes as Kaparelli is an early phase in the development of large normal faults that involves the merging of two or more faults of differing strikes, rather than the steady lengthening of a single fault segment.

e) The results from the GPS observations will help us establish both the magnitude and direction of geodetic strain and compare it with the Holocene faulting record as published in Pavlides et al., (2003) and Kokkalas et al., (in press). The orientation of the strain axes will be also compared with the configuration of the rupture zones of both the 1981 and the 1999 earthquakes (Figure 4).

ACKNOWLEDGEMENTS

This research was primarily funded by COST Action 625. We are indebted to our COST colleagues for many stimulating discussions. The NOA GPS poles were constructed at the NESTOR workshop in Pylos. We acknowledge reviews by two anonymous referees and useful comments by B. Košťák, G. Stavrakakis, S. Pavlides, I. Koukouvelas, A. Gosar, L. Piccardi, E. Tondi and V. Spina. We thank our NOA colleagues Th. Vourakis, G. Mihalettos, I. Papastamatiou, M. Papanikolaou, and A. Pirentis for help during the field trips. Many thanks are due to E. Skassis for this help with GPS instrumentation. NOA1 data are available from
http://www.epncb.oma.be/_trackingnetwork/siteinfo4onestation.php?station=NOA1_12620M001

REFERENCES

Altamini, Z., Sillard, P. and Boucher, C.: 2002, ITRF2000: A new release of the International Terrestrial Reference Frame for Earth Science applications, J. Geoph. Res. 107 (B10), 2214, doi: 10.1029/2001JB000561.

Ambraseys, N.N. and Jackson, J.A.: 1990, Seismicity and associated strain of central Greece between 1890 and 1988. Geophysical J. Int., 101, 663-708.

Armijo, R., Meyer, B., King, G.C.P., Rigo, A. and Papanastasiou, D.: 1996, Quaternary evolution of the Corinth Rift and its implications for the Late Cenozoic evolution of the Aegean. Geophys. J. Int., 126, 11–53.

Bosy, J. and Kontny, B.: 1998, Strategy of GPS data processing in local geodynamical networks, Reports on Geodesy No. 9(39), Warsaw University of Technology, Institute of Geodesy and Geodetic Astronomy, 105-113.

Bosy J., Figurski M. and Wielgosz P.: 2003, A strategy for GPS data processing in a precise local network during high solar activity. GPS Solutions, Volume 7, Number 2 Springer-Verlag, 120 – 129.

Brockmann, E.: 1996, Combination of Solutions for Geodetic and Geodynamic Applications of the Global Positioning System (GPS) PhD. dissertation, Astronomical Institute, University of Berne, Berne, Switzerland.

Cacon, S., Kontny, B., Bosy, J., Cello, G., Piccardi, L., Tondi, E., Drakatos, G. and Ganas, A.: 2005, Local geodynamic researches in Polish Sudetes and the Mediterranean region, Reports on Geodesy, No. 2 (73), 231-244.

Clarke, P.J., R.R. Davies, P.C. England, B. Parsons, H. Billiris, D. Paradissis, G. Veis, P.A. Cross, P.H. Denys, V. Ashkenazi, R. Bingley, H.-G. Kahle, M.-V. Muller and P. Briole,: 1998, Crustal strain in central Greece from repeated GPS measurements in the interval 1989-1997. Geophys. J. Int., 135(1), 195-214.

Dobrev, N., and B. Košťák,: 2000, Monitoring tectonic movements in the Simitli graben, SW Bulgaria. Engineering Geology, 57(3-4), 179-192.

Drakatos, G., Petro, L., Ganas, A., Melis, N., Košťák, B., Kontny, B., Cacon, S. and M. Stercz,: 2005, Monitoring of strain accumulation along active faults in the eastern Gulf of Corinth: Instrumentation and network setup. Acta Geodyn. Geomater., 2, No 1(137), 13 – 23.

Ganas, A., Pavlides, S. B., Sboras, S., Valkaniotis, S., Papaioannou, S., Alexandris, G. A., Plessa, A., and Papadopoulos, G. A.: 2004, Active Fault Geometry and Kinematics in Parnitha Mountain, Attica, Greece. Journal of Structural Geology, 26, 2103-2118.

Goldsworthy, M., Jackson, J. and Haines A.J.: 2002, The continuity of active fault systems in Greece. Geophysical Journal International, 148, 596-618.

Hubert, A., King, G., Armijo, R., Meyer, B. and Papanastasiou, D.: 1996, Fault Re-activation, Stress Interaction and Rupture Propagation of the 1981 Corinth Earthquake Sequence. Earth & Planet. Sci. Lett., 142, 573-585.

Hugentobler, U, Sacher, S. and Fridez, P.: 2001, Bernese GPS Software Version 4.2, Astronomical Institute, University of Berne, Switzerland.

Jackson, J.A., et al.: 1982, Seismicity, normal faulting and the geomorphological development of the Gulf of Corinth (Greece): the Corinth earthquakes of February and March 1981. Earth & Planet. Sc. Let. 57, 377– 397.

Kokkalas, S., Pavlides, S., Koukouvelas, I., Ganas, A., and Stamatopoulos, L.: in press. Paleoseismicity of the Kaparelli fault (eastern Corinth gulf): evidence for earthquake recurrence and fault behaviour. Bolletino di Geofisica Teoretica ed Applicata.

Košťák, B., and D. M. Cruden: 1990, The Moiré crack gauges on the crown of the Frank Slide. Can. Geotech. J., Vol. 27, 835-840.

Maniatis, G., Lempp, CH. and H. Heinisch: 2003, 3D strain monitoring of onshore active faults at the eastern end of the Gulf of Corinth (Greece). J. Geodynamics, 36, 95 – 102.

Pavlides, S., Koukouvelas, I., Ganas, A., Kokkalas, S., Tsodoulos, I., Stamatopoulos, L., Goyntromichou, C. and Valkaniotis, S.,: 2003, Preliminary palaeoseismological results from the Kaparelli fault (Central Greece). Geophysical Research Abstracts, Vol. 5, 07069, European Geophysical Society.

Roberts, GP. and Ganas, A.,: 2000, Fault-slip directions in central and southern Greece measured from striated and corrugated fault planes: Comparison with focal mechanism and geodetic data. Journal of Geophysical Research, 105 (B10), 23, 443-23, 462.

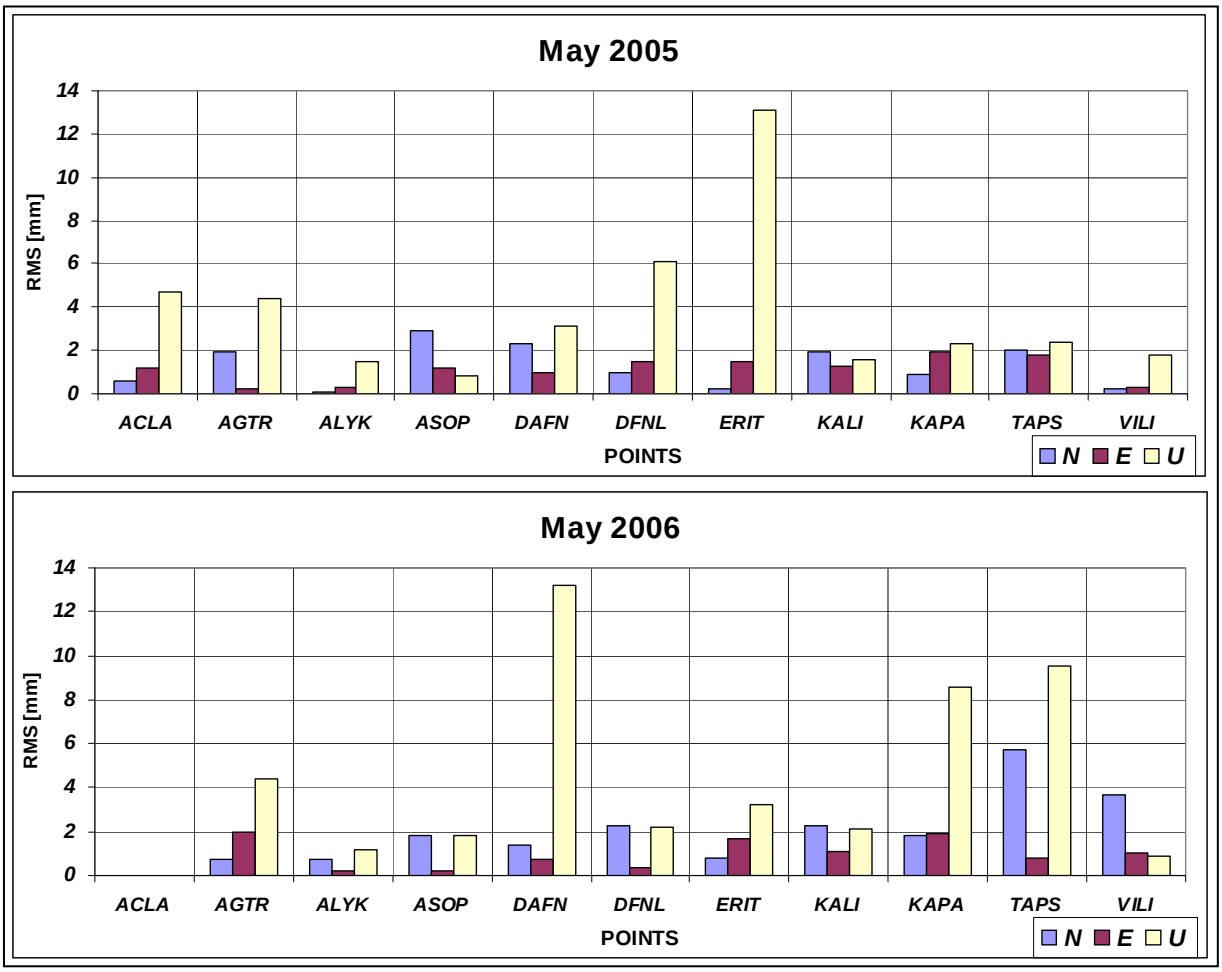

Fig. 5 The un-weighted RMS values with respect to the combined solution in mm.